

Characterization of Particulate Matter Emissions from Heavy-Duty Partially Premixed Compression Ignition with Gasoline-Range Fuels

Author, co-author (Do NOT enter this information. It will be pulled from participant tab in MyTechZone)

Affiliation (Do NOT enter this information. It will be pulled from participant tab in MyTechZone)

Abstract

In this study, the compression ratio of a commercial 15L heavy-duty diesel engine was lowered and a split injection strategy was developed to promote partially premixed compression ignition (PPCI) combustion. Various low reactivity gasoline-range fuels were compared with ultra-low-sulfur diesel fuel (ULSD) for steady-state engine performance and emissions. Specially, particulate matter (PM) emissions were examined for their mass, size and number concentrations, and further characterized by organic/elemental carbon analysis, chemical speciation and thermogravimetric analysis. As more fuel-efficient PPCI combustion was promoted, a slight reduction in fuel consumption was observed for all gasoline-range fuels, which also had higher heating values than ULSD. Since mixing-controlled combustion dominated the latter part of the combustion process, hydrocarbon (HC) and carbon monoxide (CO) emissions were only slightly increased with the gasoline-range fuels. In contrast, soot emissions were significantly reduced with the gasoline-range fuels, including a ~70% reduction in micro soot sensor measurements and a >50% reduction in smoke meter measurements. All gasoline-range fuel PM samples were also found to contain higher amount of volatile species and organic carbon fractions compared to ULSD PM samples as measured by thermogravimetric and EC-OC analyses. Various partially oxidized HC species and nitrophenolic compounds were also detected by TDP-GC-MS and CE-MS techniques, which indicated that more pronounced PPCI combustion occurred with the gasoline-range fuels. Overall similar PM oxidation behavior was observed despite the differences in reactivity and chemical properties of the fuels, although there may be some significant impacts under certain operating conditions.

Introduction

Compression ignition (CI) engines, also known as Diesel engines, offer high fuel efficiency, good driving performance, and lower carbon dioxide emissions compared to stoichiometric gasoline or natural gas engines. Conventional CI combustion is intrinsically stratified and mixing-controlled, which offers good controllability. For these reasons, CI engines are expected to remain as the primary powertrain for heavy-duty commercial transportation.

CI combustion produces different phases of pollutants, which requires a complex aftertreatment system to meet the required

emission standards. Currently, selective catalytic reduction (SCR) technology, which reduces nitrogen oxides ($\text{NO}_x = \text{NO} + \text{NO}_2$) with ammonia (NH_3) as the reductant, is most widely used due to its excellent NO_x reduction efficiency. A typical aftertreatment system using SCR technology consists of a diesel oxidation catalyst (DOC), a diesel particulate filter (DPF), SCR catalyst, and ammonia slip catalyst (ASC). Hydrocarbon (HC) and carbon monoxide (CO) are oxidized by a DOC, and particulate matter (PM) is removed by a DPF. For controlling NO_x emissions, exhaust gas recirculation (EGR) is often used to reduce the engine-out (EO) NO_x emissions to a reasonable level. The remaining NO_x is reduced by NH_3 decomposed from the aqueous urea solution, which is marketed as diesel exhaust fluid (DEF) or AdBlue, over an SCR catalyst. Excess NH_3 is then removed by an ASC.

Although PM emission can be easily controlled by a DPF, collected PM must be removed regularly in order for the DPF to remain effective. PM can be removed during normal operation through NO_2 -assisted low-temperature oxidation (also known as “passive soot oxidation”) or during periodic high-temperature oxidation (a.k.a. “active filter regeneration”). Considering the fuel economy penalty and emission control system degradation associated with high-temperature filter regeneration, diesel engine and aftertreatment systems are typically designed and operated around the DPF regeneration strategy. For example, EGR and different catalyst technologies are applied, depending on the required engine-out PM targets and the high-temperature filter regeneration frequency.

To improve the fuel economy, there has been a steady increase in EO NO_x emissions with reduced EGR among heavy-duty CI engines. This approach also produces lower PM emissions, which allows further improvement in fuel economy through longer DPF regeneration intervals. However, it requires higher NO_x reduction performance and aftertreatment system durability, which may be particularly challenging for more stringent future emission standards. Required high urea consumption also poses additional problems such as urea deposit formation inside the aftertreatment system and increased N_2O emissions. Therefore, it is imperative to control EO NO_x emissions to a manageable level and ensure the long-term durability of the aftertreatment system.

In search of both higher efficiency and lower emissions, various low temperature combustion (LTC) engine technologies, such as partially premixed compression ignition (PPCI), have been investigated for both light-duty and heavy-duty applications. Compared to ULSD, gasoline or gasoline-range fuels have higher volatility and lower

reactivity, which may help improve the air-fuel mixing and allow complete the fuel injection before auto ignition occurs. Since these fuel characteristics are desirable for LTC, the potential for very low fuel consumption and emissions from PPCI has been previously demonstrated with a diesel engine running on various gasoline-range fuels. For example, when a high octane gasoline fuel was injected late during the compression stroke of a diesel engine operating with high EGR, fuel injection could be completed before the start of combustion. As a result, fuel was partially premixed, but not fully premixed prior to the start of heat release [1,2]. Overall high combustion efficiencies have been reported when various gasoline-like low reactivity fuels were tested on diesel engines [3-14].

Previous research on PM emissions from LTC has shown the impact of combustion mode on the formation and composition of PM. For example, PM produced from diesel LTC operation was found to contain more organics and less elemental carbon compared to conventional diesel combustion (CDC) PM [14]. Diesel PPCI was also found to produce lower PM emissions, both in mass and number concentration, and smaller particles compared to CDC. However, diesel PPCI was found to increase the concentration of unregulated and toxic HC species like aldehydes and polycyclic aromatic HC [15,16]. In engine experiments with both ULSD and gasoline fuels for reactivity controlled compression ignition (RCCI) combustion operation, PM samples were found to contain mostly organic carbon and very little soot [17].

In this study, the compression ratio (CR) of a commercial 15L heavy-duty diesel engine was lowered from 19 to 17 and 16, and the split injection strategy was developed to promote the PPCI combustion. PM emissions from gasoline-range and ULSD fuels were compared for mass, size, and number at select test points, where EO NO_x level was reasonably low for the future low NO_x emission standards. In addition, the chemical composition and oxidation behavior of PM samples were examined by various analysis techniques, such as organic/elemental carbon analysis, chemical speciation and thermogravimetric analysis, to assess its potential impact on the aftertreatment system design and operation.

Experimental Setup

Engine and Instrumentation

For this study, all the experiments were conducted on a MY2013 Cummins ISX15 engine, which was controlled by Cummins' proprietary software and calibrations. The engine was equipped with a 2500-bar common rail injection system, a single-stage variable geometry turbocharger (VGT), a cooled high pressure EGR loop, and a charge air cooler (CAC). A new set of pistons were fabricated for the lower compression ratios of 17.3 and 15.7. Engine calibrations were modified for different gasoline-range fuels, while stock engine calibration was used for ULSD fuel. The specifications for the engine hardware are listed in [Table 1](#).

Table 1. Engine specifications

Engine Type	4-valve Compression Ignition
Displacement Volume	14.9 L
Number of Cylinders	6
Bore	137 mm
Stroke	169 mm

Compression Ratio	18.9, 17.3, 15.7
Diesel Fuel System	2500 bar common rail
Air System	Single-stage VGT High pressure EGR loop with cooling Charge air cooler
Engine Ratings	236 kW @ 1800 rpm 2375 N-m @ 1000 rpm

All of the engine testing was performed on an AC engine dynamometer at Aramco Research Center – Detroit. The cooling system and air system restrictions were set to the engine manufacturer's recommendations. Crank angle (CA) resolved cylinder pressure was measured using Kistler 6067C water-cooled pressure transducers installed in all of the six cylinders. High-speed data acquisition and processing was handled by AVL IndiModul hardware together with the Indicom software package. Fuel flow was measured using the AVL FuelExact Coriolis mass flow measurement unit, while intake air flow rate was measured using the AVL Flowsonix Air unit based on an ultrasonic transit time difference method. In addition, fuel return line was further cooled to prevent boiling of the gasoline-range fuels upon returning from the engine.

Fuels

In this study, various low reactivity gasoline-range fuels were tested against a US market ULSD fuel. RON 93 gasoline fuel was acquired without ethanol, while RON 60 fuel was derived directly from crude oil during the distillation process. RON 80 fuel was then prepared by blending RON 93 fuel and RON 60 fuel. ULSD, RON80 and RON93 fuels contained similar levels of aromatic hydrocarbons and low levels of sulfur. On the other hand, RON 60 fuel contained the highest fraction (~90%) of saturated hydrocarbon components, such as paraffins, isoparaffins, and naphthenes. The analysis of the fuel properties and chemical compositions was performed by Paragon Laboratories, following various ATSM standard methods. Some of the major properties of these fuels are summarized in [Table 3](#).

Table 3. Fuel properties of tested fuels

Fuel	ULSD	RON60	RON80	RON93
Research Octane Number	-	57.7	80.0	93.2
Motor Octane Number	-	58.0	74.9	84.4
Derived Cetane Number	46.6	34.1	-	-
Specific Gravity at 15.56 °C	0.845	0.715	0.724	0.734
Gross Heating Value	45.62	47.26	46.61	46.18
Net Heating Value [MJ/kg]	42.87	44.11	43.58	43.29
Carbon [wt%]	87.02	84.75	85.83	85.98
Hydrogen [wt%]	12.98	15.14	14.17	13.60
Oxygen [wt%]	<0.05	0.11	<0.05	0.42
Kinematic Viscosity	2.49	0.59	0.56	0.55
Saturates [vol%]	70.4	88.4	74.7	65.7
Olefins [vol%]	1.8	4.3	5.6	8.5
Aromatics [vol%]	27.7	7.3	19.7	24.9
Sulfur [ppm]	3.9	10.5	6.2	5.1

As shown in Table 3, kinematic viscosity was very low for the gasoline-range fuels. In order to prevent any potential problems with the fuel injection system, these fuels were doped with Infineum R650 lubricity additive at 200 ppm before use. In our earlier study, this level of additive was determined through wear scar testing, which compared the wear scar patterns of these fuels against that of ULSD fuel (ASTM D6079) [ref].

Test Conditions

In this study, steady-state emissions testing was performed at the B25 and B50 operating points, which describe low and medium load points (25 and 50%) at a fixed mid-speed (B speed) on the engine map. For example, B50 point would be 10 bar IMEP at 1375 rpm for this engine. Engine-out NOx emission level was adjusted to 1 g/kW-Hr for B25, and 2 g/kW-Hr at B50 operating point, respectively. Constant engine-out NOx emissions and CA 50, which is defined as the crank angle position where 50% of the heat is released, were maintained by adjusting the EGR rate and fuel injection timing and quantity.

A split fuel injection strategy was used for RON 80 and RON 93 fuels to facilitate earlier temperature build-up and shorten the main ignition delay, which helped the combustion stability and prevented excessive MPRR. The fuel injection quantity split between the two injections was determined based on overall fuel efficiency, MPRR, and smoke, etc., as discussed in our earlier study [2018 SAE]. The details of the engine operation used in this study are listed in Table 2.

Table 2. Engine operation parameters

(A) B25 operating point

CR	15.7		17.3	
Fuel	ULSD	RON 80	ULSD	RON 60
Injection Strategy	Single	Split	Single	
Injection Pressure [bar]	1300	800	1300	
Split Ratio	N/A	50:50	N/A	
SOIp [°ATDC]	-6.8	-30	-9.5	-8.2
CA50 [°ATDC]	6.4	5.8		4.2
VGT [%]	60.0	56.2	59.5	57.2
EGR [%]	75	75	65	65

(B) B50 operating point

CR	15.7		17.3		18.9	
Fuel	ULSD	RON 93	ULSD	RON 60	ULSD	RON 93
Injection Strategy	Single	Split	Single		Single	Split
Injection Pressure [bar]	1450					
Split Ratio	N/A	40:60	N/A		N/A	10:90

SOIp [°ATDC]	-9	-30	-10.2	-10.2	-9	-8
CA50 [°ATDC]	7.1	6.9		5.4	6.7	6.4
VGT [%]	55.7	54.6	55.7	55.8	58.4	59.0
EGR [%]	50	50	40	40	40	40

Emissions Measurement

Engine-out exhaust emissions were measured by Horiba Mexa-7500D emissions bench. NOx and HC emissions were measured by a standard heated chemiluminescence detector (CLD) and a flame ionization detector (FID), respectively. CO and intake/exhaust CO2 emissions were measured using non-dispersive infrared (NDIR) instruments. A paramagnetic detector (PMD) was used to measure the exhaust O2 concentration. For PM emissions, a smoke meter (SMK, AVL 415SE) and a micro soot sensor (MSS, AVL 483) were used to measure filtered smoke number (FSN) and soot concentration (mg/m³), respectively. PM size distributions were also measured by a particle size analyzer (TSI EEPS 3090) after exhaust conditioning by a dual-stage dilution system (Dekati DEED).

Particulate Matter Sampling and Analysis

PM samples were collected by a partial flow dilution gravimetric PM sampler (AVL 478), which includes a single-stage dilution system and sampling manifold inside a heated oven. For this study, the dilution ratio was lowered to 3 to accelerate the PM collection. The temperature of the heated oven was maintained at 47°C to minimize the volatilization of organics from the PM samples and to prevent the condensation of water vapor onto the PM samples. PM samples were collected on pre-fired, 47-mm diameter quartz-fiber filters (QFF, Advantec) as well as TX40 filters (Pallflex Emfab).

Overall composition and oxidation behavior of PM samples were examined by thermogravimetric analysis (TGA) technique. Samples for TGA were cut from the QFF using a 6-mm diameter hole punch. Two 6-mm disks from the same filter were measured together in each TGA analysis. Temperature-programmed oxidation (TPO) experiment was performed using a TA Instruments Q500 TGA. Samples were first held at 50 °C for 20 minutes in N₂, and then heated in dry air at 5 °C/min to 800 °C.

For elemental carbon (EC) and organic carbon (OC) analysis, a primary QFF and a set of Teflon membrane and filter (TF, Measurement Tech Lab) followed by a second QFF were used. Both the primary and secondary QFF were analyzed for EC-OC content using the NIOSH method by Sunset Laboratory [7]. OC was first removed in oxygen-free helium, and the remaining EC was oxidized in 2% O₂ in Helium. The measured organics absorbed on the secondary QFF were subtracted from the primary QFF OC content to correct for filter adsorption artifacts [8,9].

Non-polar HC species, such as fuel and oil, on PM samples were examined using thermal desorption-gas chromatography-mass spectrometry (TD/GC/MS), developed at Oak Ridge National Laboratory. Samples were collected on 2-mm diameter punch outs.... Oven temp ramp to 325 °C... (to be written by ORNL)

In addition, partially oxidized polar HC species, such as carboxylic acid and phenols, were examined by capillary electrophoresis-mass spectrometry (CE/MS). Samples were extracted by aqueous methanol solution,... (to be written by ORNL)

CO ₂ [%]	8.9	8.2		7.8
MSS [mg/m ³]	11.4	3.7	29.0	2.5
SMK [FSN]	0.78	0.33	1.59	0.19

Results and Discussion

Effects of Fuel and Combustion on Engine Performance and Emissions

The effects of fuels and combustion mode on engine performance and emissions are summarized in Table 4. Steady-state performance and emissions were measured at the B25 and B50 operating points. As listed in Table 2, some of the engine parameters were adjusted for different fuels to maintain constant EO NO_x emissions and CA 50. As more fuel-efficient premixed combustion was promoted with low reactivity gasoline-range fuels, which also had higher heating values (shown in Table 3), a slight reduction in brake specific fuel consumption (BSFC) and a slight increase in brake thermal efficiency (BTE) were observed compared to ULSD fuel.

Although high HC and CO emissions are typically produced from premixed combustion, relatively small increase in HC and CO emissions were observed in our study. Since pilot SOI was advanced only to -30 °ATDC because of the controller's limitation, most of injected fuel was contained inside the piston bowl. As a result, although premixed combustion was promoted, mixing-controlled diffusion combustion still dominated the latter part of combustion process, reducing the HC and CO emissions. For this reason, higher HC and CO emissions observed for RON 80 and RON 93 fuels may be attributed to their low reactivity compared to RON 60 and ULSD fuels.

As partially premixed combustion was promoted, PM emissions were significantly reduced for all three gasoline-range fuels. For example, soot emissions measured by MSS showed ~70% reduction for three gasoline-range fuels compared to ULSD fuels, while smoke meter readings showed >50% reduction. Interestingly, PM reduction was still observed with RON 93 fuel at the CR of 18.7. Since similar ignition delay (defined as time between EOI and CA5) was observed for RON 93 and ULSD fuels in our previous study, the cylinder pressure and temperature might have been sufficiently high enough to suppress any effects of fuel reactivity during the combustion. This suggests that the high volatility and lower reactivity of gasoline-range fuels can still help improve the fuel-air mixing before the start of combustion even at a relatively high CR of 18.7.

Table 4. Engine performance and engine-out emissions

(A) B25 operating point

CR	15.7		17.3	
	ULSD	RON 80	ULSD	RON 60
Fuel	ULSD	RON 80	ULSD	RON 60
BSFC [g/kWhr]	222	216		212
BTE [%]	37.8	38.4		38.5
BSNO _x [g/kWhr]	1.11	1.17	1.04	1.09
NO _x [ppm]	132	140	141	145
THC [ppm]	39	179		90
CO Low [ppm]	178	804		172

(B) B50 operating point

CR	15.7		17.3		18.9	
	ULSD	RON 93	ULSD	RON 60	ULSD	RON 93
Fuel	ULSD	RON 93	ULSD	RON 60	ULSD	RON 93
BSFC [g/kWhr]	204	200		195	199	198
BTE [%]	41.1	41.5		41.9	42.3	42.1
BSNO _x [g/kWhr]	2.01	2.15	2.17	2.05	2.06	2.16
NO _x [ppm]	291	309	350	335	363	376
THC [ppm]	23	62		38	29	47
CO Low [ppm]	188	461		126	359	435
CO ₂ [%]	9.7	9.4		9.5	10.1	10.1
MSS [mg/m ³]	19.3	6.5	16.7	6.0	31.4	20.7
SMK [FSN]	1.17	0.52	1.05	0.44	1.71	1.28

Effects of Fuel and Combustion on Particulate Matter Size and Number

Since a huge reduction in PM emissions was observed for RON 60 fuel at the B25 operating point, PM size distribution was further examined using the EEPS at the dilution ratio of 88. Typically, most particles are formed in the nanoparticle region during the combustion. As these particles cool down in the exhaust, they agglomerate and form larger particles, which reduces the total number concentration. As shown in Figure 1(A), RON 60 PM particles were mostly found in the regions of nanoparticles and ultrafine particles (10-100 nm) compared to ULSD PM particles.

Interestingly, similar particle size and concentration were observed for both fuels at the B50 operating point (shown in Figure 1(B)), where ~30% reduction in PM emissions were measured by MSS and SMK for RON 60 fuel. When PM mass was estimated based on the particle size distribution using published soot density values for gasoline and diesel PM, a large discrepancy was seen compared to MSS measurement. This suggests the RON 60 PM particles may be much less compact than ULSD PM particles even when mixing-controlled combustion was more prevalent at this operating point.

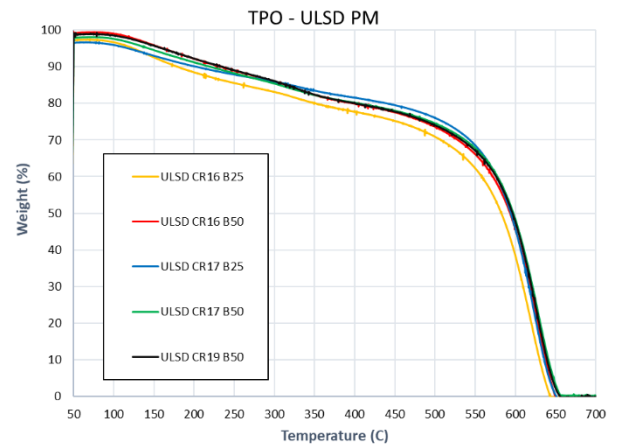
(A) B25 operating point

$$(m_{PM(x)}/m_{PMt}) * 100 = \%m_{PM(x)} \quad (3)$$

As shown in Figure 2, volatile HC species are first removed as the temperature was raised, before the oxidation of PM commences around 600 °C. Not surprisingly, all ULSD PM samples collected on QFF showed near identical TPO profile, indicating the little impact of compression ratio on the composition and oxidation behavior. On the other hand, all the gasoline-range fuel PM samples showed higher volatile content and much faster oxidation behavior. In particular, RON 60 PM samples contain as high as 45% volatiles and much faster oxidation.

Interestingly, RON 93 PM sample collected at the B50 operating point and CR of 18.7 was found to contain ~25% volatiles, similar to ULSD PM, yet still show faster oxidation behavior. As noted earlier, the impacts of fuel reactivity may be limited under high cylinder pressure and temperature, but the high volatility and lower reactivity of gasoline-range fuels can still influence the PM oxidation.

(A) ULSD fuels



(B) Gasoline-range fuels

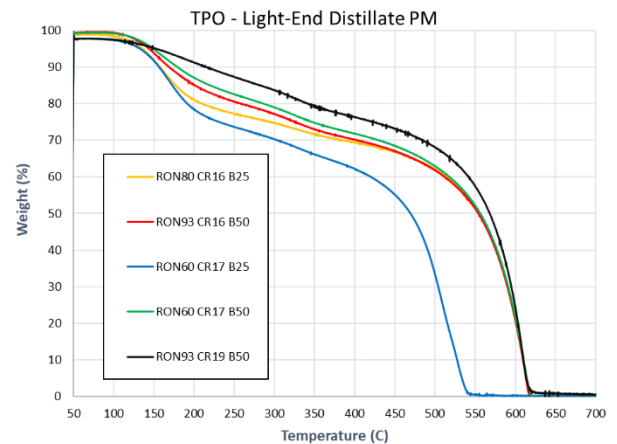
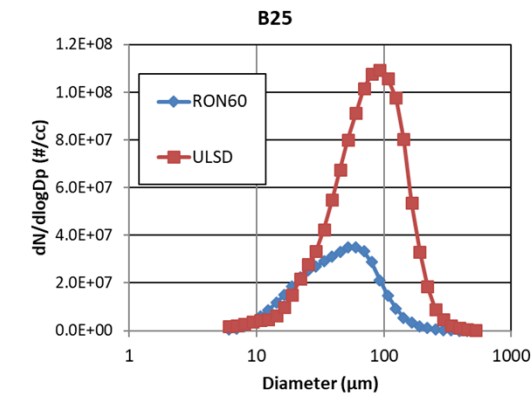


Figure 2. Normalized PM mass loss during TGA

The derivatives of the normalized PM weight loss as a function of temperature are shown in Figure 3. These curves compare the reactivity and peak oxidation temperature of PM samples. Just like



(B) B50 operating point

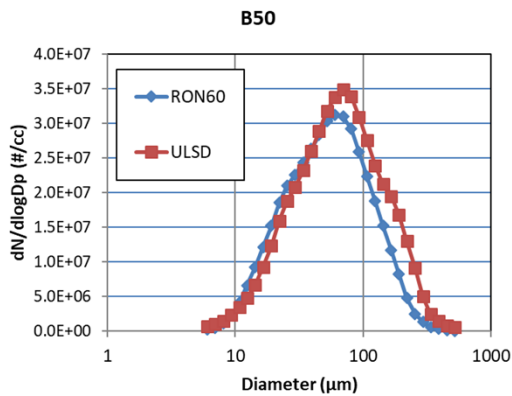


Figure 1. PM size distribution

Effects of Fuel and Combustion on Particulate Matter Oxidation

Considering the importance of PM oxidation in the design and operation of DPF system, the impacts of fuel and combustion on the oxidation behavior was further examined by the thermogravimetric analysis (TGA). Samples were cut from the QFF, and temperature-programmed oxidation (TPO) experiment was performed to measure the weight change as a function of temperature. Because the QFF weight could not be measured accurately, the collected PM mass was estimated according to Equation (1). It was assumed that all PM was oxidized during the TPO, so that the initial TGA filter weight (m_{Fi}) minus the final TGA filter weight (m_{Ff}) could be used to calculate the total mass of PM loaded on the weighing pan during each TGA run (m_{PMt}). Because ash content in PM could not be separately examined, its content was counted as part of m_{Ff} . Following Equations (2) and (3), the sample weight measurement ($m_{PM(x)}$) was normalized as $\%m_{PM(x)}$, resulting in 100% weight loss at the end of the experiment.

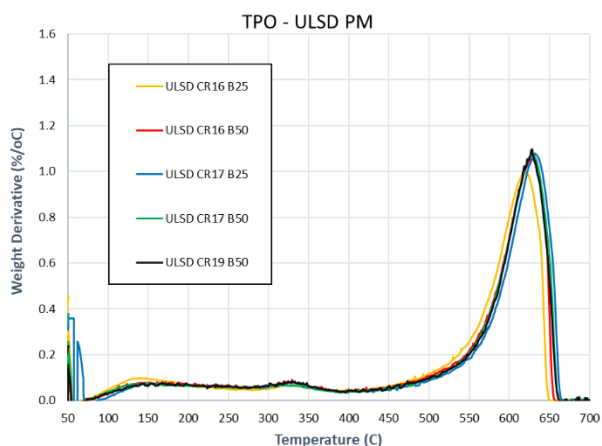
$$m_{Fi} - m_{Ff} = m_{PMt} \quad (1)$$

$$m_{F(x)} - m_{Ff} = m_{PM(x)} \quad (2)$$

Figure 2, all ULSD PM samples showed near identical profile with peak oxidation temperature around 620-630 °C regardless of compression ratios. On the other hand, all the gasoline-range fuel PM samples showed more pronounced low temperature mass changes as well as lower peak oxidation temperatures. The low temperature peaks suggest the presence of un-burned fuel-component HC (~150 °C) and the soluble organic fraction (SOF) of the PM (~325 °C). The main inflection point of the TPO experiment, which suggests the peak oxidation temperature, was always slightly lower and sharper for gasoline-range PM (~610 °C), including RON 93 CR19 PM samples.

Interestingly, RON 60 PM samples collected at the B25 operating point showed much lower peak oxidation temperature (510-525 °C), but not at the B50 operating point. RON 60 fuel contained mostly saturated hydrocarbons and little aromatic hydrocarbons. This suggests that overall PM oxidation behavior appear to be similar despite the differences in reactivity and chemical composition of fuels, although there may be some significant impacts under certain conditions.

(A) ULSD fuel



(B) Gasoline-range fuels

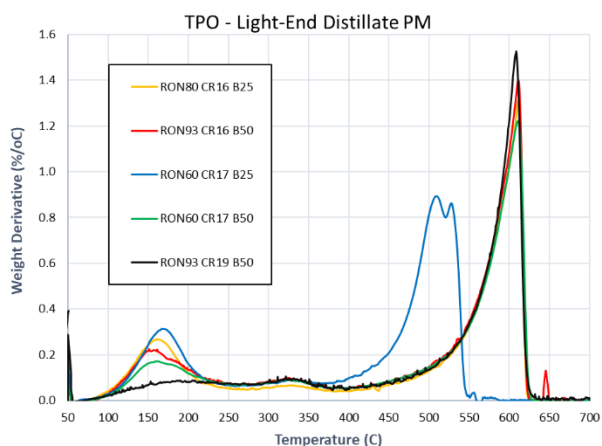


Figure 3. Derivative of the PM mass loss as a function of temperature

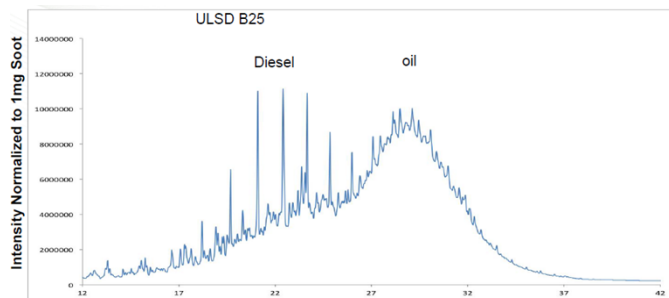
Effects of Fuel and Combustion on Particulate Matter Chemistry

Some of the PM samples were further analyzed to assess the effects of fuels and combustion modes on the chemical composition in terms of elemental carbon (EC) and organic carbon (OC). As shown in Table 5, it was found that gasoline-range PM samples were found to contain higher fraction of OC compared to ULSD PM samples. This suggests that the significant reduction in the total PM emissions with gasoline-range fuels can be primarily attributed to the reduction in EC, which can complement the oxidation behavior and particle size distribution discussed in the earlier sections. As OC can be easily oxidized over DOC and DPF catalysts, higher fraction of OC may help reduce the frequency and severity of high-temperature DPF regeneration, which is beneficial for the fuel economy and aftertreatment system durability.

Table 5. EC and OC contents in PM samples

Fuel	CR	Test Point	EC:OC ratio
ULSD	15.7	B25	0.78:0.22
		B50	0.77:0.23
	17.3	B25	
		B50	
RON 80	15.7	B25	0.67:0.33
RON 60	17.3	B25	
RON 60		B50	
RON 93	15.7	B50	0.69:0.31

Some of the hydrocarbon species present on PM samples were further examined by thermal desorption-gas chromatography-mass spectrometry (TD/GC/MS) and capillary electrophoresis-mass spectrometry (CE/MS). As indicated by TPO experiment and EC-OC analysis, PM samples contain various HC species, including combustion products and engine oil. As shown in Figure 4, the presence of non-polar HC species like fuel-component HC and oil were detected by TDU/GC/MS. All ULSD samples were found to contain both fuel and oil component HC species, while RON 80 and RON 93 PM samples were found to contain nitrogenated HC compounds and oil component HC species. Little fuel-component HC species were found in the gasoline-range PM samples possibly because of their high volatility.



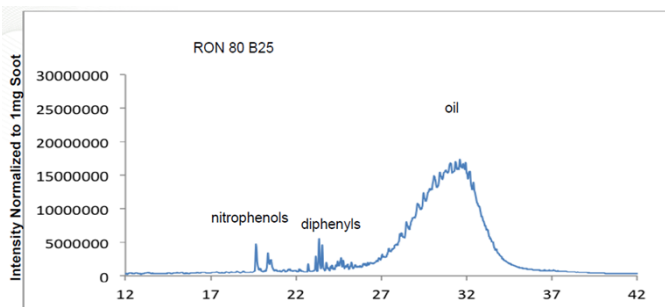


Figure 4. Non-polar HC species detected by TDU-GC-MS for ULSD and RON 80 PM samples

In addition, the presence of partially oxidized polar HC species of low volatility were examined by capillary electrophoresis-mass spectrometry (CE/MS). As shown in Figure 5, gasoline-range PM samples were found to contain carboxylic acids and nitrophenolic compounds, whereas ULSD PM samples were found to contain none of these species. Since NO₂ fraction in the exhaust tend to be higher during the low-temperature combustion, it is mostly likely that these nitrogenated HC species have been formed between fuel-component HC and NO₂. These nitrogen-containing species may act as nitrogen sink and help with the soot oxidation at lower temperature. (We can talk about perceived high NO_x conversion, but that can be possible only at very higher amount, don't you think?)

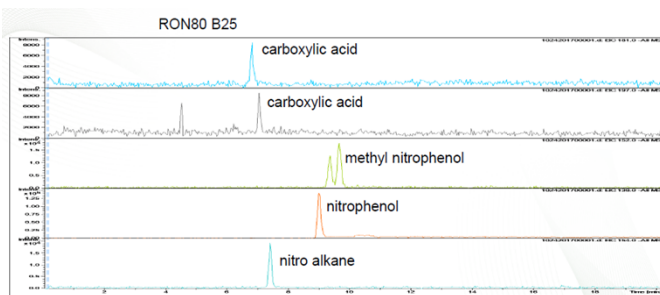


Figure 5. Polar HC species detected by CE/GC for RON 80 PM sample

Table for NO₂ fraction?

Summary/Conclusions

References

1. The Outlook for Energy: A View to 2040, Exxon Mobil, 2016, corporate.exxonmobil.com/en/energy/energy-outlook.
2. U.S. Energy Information Administration, "International Energy Outlook 2014: World Petroleum and Other Liquid Fuels," 2014.
3. World Energy Council, "World Energy Scenarios" Global Transport Scenarios 2050," 2011.
4. Zhang, Y., Kumar, P., Traver, M., Cleary, D., "Conventional and Low Temperature Combustion using Naphtha Fuels in a Multi-Cylinder Heavy-Duty Diesel Engine," SAE Technical Paper 2016-01-0764, 2016, doi:10.4271/2016-01-0764.

5. Akihama, K., Kosaka, H., Hotta, Y., Nishikawa, K., "An Investigation of High Load (Compression Ignition) Operation of the "Naphtha Engine" - a Combustion Strategy for Low Well-to-Wheel CO₂ Emissions," *SAE Int. J. Fuels Lubr.* 1(1):920-932, 2009, doi:10.4271/2008-01-1599.
6. Rose, K., Cracknell, R., Rickeard, D., Ariztegui, J., "Impact of Fuel Properties on Advanced Combustion Performance in a Diesel Bench Engine and Demonstrator Vehicle," SAE Technical Paper 2010-01-0334, 2010, doi:10.4271/2010-01-0334.
7. NIOSH Manual of Analysis Methods, "Diesel Particulate Matter (as Elemental Carbon)," NIOSH Method 5040, Rev. Mar. 2003.
8. Curran, S., Prikhodko, V., Cho, K., Sluder, S., Parks, J., Wagner, R., "In-Cylinder Fuel Blending of Gasoline/Diesel for Improved Efficiency and Lowest Possible Emissions on a Multi-Cylinder Light-Duty Diesel Engine," SAE technical paper 2010-01-2206, 2010, doi:10.4271/2010-01-2206
9. Storey, J.E.M., Curran, S.J., Lewis, S.A., Barone, T.L., Dempsey, A.B., Moses-DeBusk, M., Hanson, R.M., Prikhodko, V.Y., Northrop, W.F., "Evolution of Current Understanding of Physicochemical Characterization of Particulate Matter from Reactivity Controlled Compression Ignition Combustion on a Multicylinder Light-Duty Engine," *Int. J. Engine Res.* Prepublished August 4, 2016, doi: 10.1177/1468087416661637
10. Reijnders, J., Boot, M., de Goey, P., "Impact of Aromaticity and Cetane Number on the Soot-NO_x Trade-Off in Conventional and Low Temperature Combustion," *Fuel*, 186:24-34, 2016, doi:10.1016/j.fuel.2016.08.009
11. Yezerets, A., Currier, N., Eadler, H., Suresh, A., Madden, P., Branigin, M., "Investigation of the Oxidation Behavior of Diesel Particulate Matter," *Catal. Today*, 88: 17-25, 2003, doi:10.1016/j.cattod.2003.08.003

1. Kalghatgi, G., "Auto-Ignition Quality of Practical Fuels and Implications for Fuel Requirements of Future SI and HCCI Engines," SAE Technical Paper 2005-01-0239, 2005, doi:10.4271/2005-01-0239.
2. Johansson, B., "High-Load Partially Premixed Combustion in a Heavy-Duty Diesel Engine", Diesel Engine Emissions Reduction (DEER) Conference Presentations, 2005, Chicago, IL.
3. Risberg, P., Kalghatgi, G., Ångström, H., and Wåhlin, F., "Auto-ignition quality of Diesel-like fuels in HCCI engines," SAE Technical Paper 2005-01-2127, 2005, doi:10.4271/2005-01-2127.
4. Kalghatgi, G., Risberg, P., and Ångström, H., "Advantages of Fuels with High Resistance to Auto-ignition in Late-injection, Low-temperature, Compression Ignition Combustion," SAE Technical Paper 2006-01-3385, 2006, doi:10.4271/2006-01-3385.
5. Kalghatgi, G., Risberg, P., and Ångström, H., "Partially Premixed Auto-Ignition of Gasoline to Attain Low Smoke and Low NO_x at High Load in a Compression Ignition Engine and Comparison with a Diesel Fuel," SAE Technical Paper 2007-01-0006, 2007, doi:10.4271/2007-01-0006.
6. Kalghatgi, G., "Low NO_x Low Smoke Operation of a Diesel Engine using Gasoline-Like Fuels", ASME 2009 International Combustion Engine Division Spring Technical Conference, ICES2009-76034, 2009.
7. Manente, V., Johansson, B., and Tunestal, P., "Partially Premixed Combustion at High Load using Gasoline and Ethanol, a Comparison with Diesel," SAE Technical Paper 2009-01-0944, 2009, doi:10.4271/2009-01-0944.
8. Manente, V., Tunestal, P., Johansson, B., and Cannella, W., "Effects of Ethanol and Different Type of Gasoline Fuels on Partially Premixed Combustion from Low to High Load," SAE Technical Paper 2010-01-0871, 2010, doi:10.4271/2010-01-0871.

9. Weall, A. and Collings, N., "Gasoline Fuelled Partially Premixed Compression Ignition in a Light Duty Multi Cylinder Engine: A Study of Low Load and Low Speed Operation," *SAE Int. J. Engines* 2(1):1574-1586, 2009, doi:[10.4271/2009-01-1791](https://doi.org/10.4271/2009-01-1791).
10. Dempsey, A. and Reitz, R., "Computational Optimization of a Heavy-Duty Compression Ignition Engine Fueled with Conventional Gasoline," *SAE Int. J. Engines* 4(1):338-359, 2011, doi:[10.4271/2011-01-0356](https://doi.org/10.4271/2011-01-0356).
11. Ra, Y., Loeper, P., Reitz, R., Andrie, M. et al., "Study of High Speed Gasoline Direct Injection Compression Ignition (GDICI) Engine Operation in the LTC Regime," *SAE Int. J. Engines* 4(1):1412-1430, 2011, doi:[10.4271/2011-01-1182](https://doi.org/10.4271/2011-01-1182).
12. Ra, Y., Loeper, P., Andrie, M., Krieger, R. et al., "Gasoline DICI Engine Operation in the LTC Regime Using Triple- Pulse Injection," *SAE Int. J. Engines* 5(3):1109-1132, 2012, doi:[10.4271/2012-01-1131](https://doi.org/10.4271/2012-01-1131).
13. Sang, W., and Cheng, W., Maria, A., "The Nature of Heat Release in Gasoline PPCI Engines," SAE Technical Paper [2014-01-1295](https://doi.org/10.4271/2014-01-1295), 2014, doi:[10.4271/2014-01-1295](https://doi.org/10.4271/2014-01-1295).
14. Chang, J., Kalghatgi, G., Amer, A., Adomeit, P., "Vehicle Demonstration of Naphtha Fuel Achieving Both High Efficiency and Drivability with Euro6 Engine-Out NOx Emissions," *SAE Int. J. Engines* 6(1):101-119, 2013, doi:[10.4271/2013-01-0267](https://doi.org/10.4271/2013-01-0267).
15. Sellnau, M., Sinnamon, J., Hoyer, K., and Husted, H., "Gasoline Direct Injection Compression Ignition (GDICI) - Diesel-like Efficiency with Low CO2 Emissions," *SAE Int. J. Engines* 4(1):2010-2022, 2011, doi:[10.4271/2011-01-1386](https://doi.org/10.4271/2011-01-1386).
16. Sellnau, M., Sinnamon, J., Hoyer, K., and Husted, H., "Full-Time Gasoline Direct-Injection Compression Ignition (GDICI) for High Efficiency and Low NOx and PM," *SAE Int. J. Engines* 5(2):300-314, 2012, doi:[10.4271/2012-01-0384](https://doi.org/10.4271/2012-01-0384).
17. Sellnau, M., Sinnamon, J., Hoyer, K., Kim, J. et al., "Part-Load Operation of Gasoline Direct-Injection Compression Ignition (GDICI) Engine," SAE Technical Paper [2013-01-0272](https://doi.org/10.4271/2013-01-0272), 2013, doi:[10.4271/2013-01-0272](https://doi.org/10.4271/2013-01-0272).
18. Sellnau, M., Foster, M., Hoyer, K., Moore, W. et al., "Development of a Gasoline Direct Injection Compression Ignition (GDICI) Engine," *SAE Int. J. Engines* 7(2):2014, doi:[10.4271/2014-01-1300](https://doi.org/10.4271/2014-01-1300).
19. Sellnau, M., Moore, W., Sinnamon, J., Hoyer, K. et al., "GDICI Multi-cylinder Engine for High Fuel Efficiency and Low Emissions," *SAE Int. J. Engines* 8(2):775-790, 2015, doi:[10.4271/2015-01-0834](https://doi.org/10.4271/2015-01-0834).
20. Kolodziej, C., Sellnau, M., "Operation of a Gasoline Direct Injection Compression Ignition Engine on Naphtha and E10 Gasoline Fuels," SAE Technical Paper [2016-01-0759](https://doi.org/10.4271/2016-01-0759), 2016, doi:[10.4271/2016-01-0759](https://doi.org/10.4271/2016-01-0759).
21. Sellnau, M., Foster, M., Moore, W., Sinnamon, J., Hoyer, K., Klemm, W., "Second Generation GDICI Multi-Cylinder Engine for High Fuel Efficiency and US Tier 3 Emissions," SAE Technical Paper [2016-01-0760](https://doi.org/10.4271/2016-01-0760), 2016, doi:[10.4271/2016-01-0760](https://doi.org/10.4271/2016-01-0760).
22. SGS Group, "SGS Worldwide Fuel Survey (WWFS)," Summer 2013, Winter 2013/2014.
23. Cho, K., Latimer, E., Lorey, M., Cleary, D., "Gasoline Fuels Assessment for Delphi's Second Generation Gasoline Direct-Injection Compression Ignition (GDICI) Multi-Cylinder Engine," SAE Technical Paper [2017-01-0743](https://doi.org/10.4271/2017-01-0743), 2017.
24. Storey, J. M., Barone, T., Norman, K., and Lewis, S., "Ethanol blend effects on direct injection spark- ignition gasoline vehicle particulate matter emissions," *SAE Int. J. Fuels Lubr.*, vol. 3, pp. 650-659, 2010, doi:[10.4271/2010-01-2129](https://doi.org/10.4271/2010-01-2129).
25. Storey, JME, TL Barone, JF Thomas, and SP. Huff, 2012. "Exhaust Particle Characterization for Lean and Stoichiometric DI Vehicles Operating on Ethanol-Gasoline Blends," SAE Technical Paper Series [2012-01-0437](https://doi.org/10.4271/2012-01-0437), 2012, doi:[10.4271/2012-01-0437](https://doi.org/10.4271/2012-01-0437).
26. Storey, JME, Lewis, SA, Szybist, JP., Thomas, JF., Barone, T.L., Eibl, MA, and Kaul, B, "Novel Characterization of GDI Engine Exhaust for Gasoline and Mid-Level Gasoline-Alcohol Blends," *SAE Int. J. Fuels Lubr.*, vol. 7, pp. 1-8, 2014, doi:[10.4271/2014-01-1606](https://doi.org/10.4271/2014-01-1606).
27. Storey, J., Domingo, N., Lewis, S., and Irick, D., "Analysis of Semivolatile Organic Compounds in Diesel Exhaust Using a Novel Sorption and Extraction Method," SAE Technical Paper [1999-01-3534](https://doi.org/10.4271/1999-01-3534), 1999, doi:[10.4271/1999-01-3534](https://doi.org/10.4271/1999-01-3534).
28. Koci, C., Ra, Y., Krieger, R., Andrie, M. et al., "Detailed Unburned Hydrocarbon Investigations in a Highly-Dilute Diesel Low Temperature Combustion Regime," *SAE Int. J. Engines* 2(1):858-879, 2009, doi:[10.4271/2009-01-0928](https://doi.org/10.4271/2009-01-0928).
29. Storey, S.J., Curran, S., Lewis, S., et al., "Evolution and current understanding of physicochemical characterization of particulate matter from reactivity controlled compression ignition combustion on a multi-cylinder light-duty engine", *Int. J. Engine Res.*, 2016, doi:[10.1177/1468087416661637](https://doi.org/10.1177/1468087416661637).

Contact Information

Jong Lee
 Aramco Research Center – Detroit
 46535 Peary Court
 Novi, MI 48377 USA
jong.lee@aramcoservices.com

Acknowledgments

The authors appreciate all the support provided by the staff at the Aramco Research Center – Detroit, and especially thank Steven Sommers and Michael Zimmermann (Aramco Research Center) for the test cell operation and data collection. The authors also gratefully acknowledge all the technical support provided by Sriram Popuri and Suk-Min Moon for engine controls (Cummins).

Definitions/Abbreviations

ATDC	After Top Dead Center
ASC	Ammonia Slip Catalyst
BSFC	Brake Specific Fuel Consumption
BTE	Brake Thermal Efficiency
CA	Crank Angle
CAC	Charge Air Cooler
CAD	Crank Angle Degree
CN	Cetane Number
CO	Carbon Monoxide

CR	Compression Ratio	NOx	Nitrogen Oxides
DOC	Diesel Oxidation Catalyst	OC	Organic Carbon
DEF	Diesel Exhaust Fluid	PM	Particulate Matter
DPF	Diesel Particulate Filter	PPCI	Partially Premixed Compression Ignition
EC	Elemental Carbon	QFF	Quartz Fiber Filter
EGR	Exhaust Gas Recirculation	RMC	Ramped Mode Cycle
EO	Engine-Out	RON	Research Octane Number
EPA	Environmental Protection Agency	SCR	Selective Catalytic Reduction
FSN	Filter Smoke Number	SMK	Smoke meter
FTIR	Fourier-Transform Infrared	SOF	Soluble Organic Fraction
HC	Hydrocarbon	TF	Teflon filter
HRR	Heat Release Rate	ULSD	Ultra-Low-Sulfur Diesel fuel
ID	Ignition Delay	VGT	Variable Geometry Turbocharger
IMEP	Indicated Mean Effective Pressure		
MON	Motor Octane Number		
MSS	Micro Soot Sensor		
MY	Model Year		
NIOSH	Nat'l Inst. for Occupational Safety & Health		
NO	Nitric Oxide		

Appendix

The Appendix is one-column. If you have an appendix in your document, you will need to insert a continuous page break and set the columns to one. If you do not have an appendix in your document, this paragraph can be ignored and the heading and section break deleted.